ACS EARTH AND SPACE CHEMISTRY

http://pubs.acs.org/journal/aesccq

Article

Boron Adsorption to Ferrihydrite with Implications for Surface Speciation in Soils: Experiments and Modeling

Elise Van Eynde,* Juan C. Mendez, Tjisse Hiemstra, and Rob N. J. Comans

Cite This: *ACS Earth Space Chem.* 2020, 4, 1269−1280

Read Online

ACCESS | Metrics & More | Article Recommendations | Supporting Information

ABSTRACT: The adsorption and desorption of boric acid onto reactive materials such as metal (hydr)oxides and natural organic matter are generally considered to be controlling processes for the leaching and bioavailability of boron (B). We studied the interaction of B with ferrihydrite (Fh), a nanosized iron (hydr)oxide omnipresent in soil systems, using batch adsorption experiments at different pH values and in the presence of phosphate as a competing anion. Surface speciation of B was described with a recently developed multisite ion complexation (MUSIC) and charge distribution (CD) approach. To gain insight into the B adsorption behavior in whole-soil systems, and in the relative contribution of Fh in particular, the pH-dependent B speciation was evaluated for soils with representative amounts of ferrihydrite, goethite, and organic matter. The pH-dependent B adsorption envelope of ferrihydrite is bell-shaped with a maximum around pH 8−9. In agreement with spectroscopy, modeling suggests formation of a trigonal bidentate complex and an additional outer-sphere complex at low to neutral pH values. At high pH, a tetrahedral bidentate surface species becomes important. In the presence of phosphate, B adsorption decreases strongly and only formation of the outer-sphere surface complex is relevant. The pH-dependent B adsorption to Fh is rather similar to that of goethite. Multisurface modeling predicts that ferrihydrite may dominate the B binding in soils at low to neutral pH and that the relative contribution of humic material increases significantly at neutral and alkaline pH conditions. This study identifies ferrihydrite and natural organic matter (i.e., humic substances) as the major constituents that control the B adsorption in topsoils.

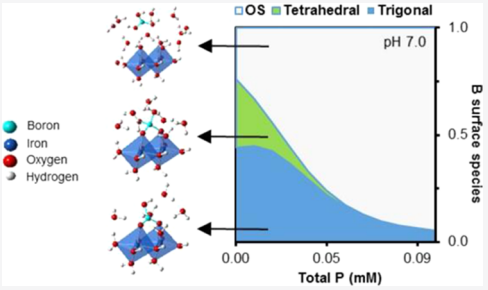

KEYWORDS: *boron, ferrihydrite, CD-MUSIC modeling, humic acid, goethite*

INTRODUCTION

Boron (B) is an essential micronutrient to sustain plant growth and development.[1] Plants take up B from the soil solution as boric acid ($B(OH)_3^0$), which is the dominant B species in the soil solution at pH values below 9.[2] The concentration of B in the soil solution usually varies in the range between 1 and 300 μM.[3] Boron deficiencies in crop production have been reported in many parts of the world, especially in strongly weathered acidic soils and alkaline soils.[4] However, boron toxicity has also been reported[5,6] to reduce crop growth.

The bioavailability, toxicity, and mobility of boron and its loss by leaching[7−9] are related to the solution concentration of B. It has been stated that the B concentration in the soil solution depends on the interaction of B with soil mineral surfaces as well as with natural organic matter (OM).[10−13] In the literature, B adsorption has been studied for various Fe (hydr)oxides including goethite[14] and ferrihydrite (Fh).[15−17] The latter material was found to be a key variable in explaining the pH-dependent B adsorption of soils.[18] Ferrihydrite is a nanomaterial that is ubiquitous in natural soil systems.[19] Due to its small particle size and corresponding large specific surface area (SSA), it has a significantly higher adsorption capacity than other Fe (hydr)oxides, making this mineral particularly relevant for elucidating the B adsorption properties of soils.

Surface complexation modeling (SCM) can be used to understand, identify, and predict interactions of ions with reactive mineral and organic surfaces and, when applied in a multisurface approach, to comprehend the speciation of major and trace elements in soil environments and the processes that affect their bioavailability.[20] To date, B adsorption to Fh has been modeled using the diffuse layer model (DLM)[21] or, more commonly, the constant capacitance model (CCM).[15,22] Both models simplify the mineral−solution interface to a single surface plane in which inner-sphere complexes reside, while outer-sphere (OS) complexation cannot explicitly be considered.[23]

A more realistic physical representation of the interface is a double-layer model in which surface charge and counter-charge are separated by a Stern layer.[24] This approach can be further refined by introducing for inner-sphere surface complexes the concept of charge distribution (CD).[25] In combination, this

Received: March 26, 2020
Revised: July 23, 2020
Accepted: July 29, 2020
Published: July 29, 2020

https://dx.doi.org/10.1021/acsearthspacechem.0c00078
ACS Earth Space Chem. 2020, 4, 1269−1280

leads to an improved calculation of the electrostatic energy of ion adsorption. For Fh, surface complexation modeling can be further improved using a realistic set of reactive sites and corresponding site densities that are based on a surface structural approach,[26,27] rather than using a set of hypothetical reactive sites with a virtual site density. Such an advancement is presently possible due to our improved insights into the structure of Fh.[28−30]

Another aspect of improving our understanding of the ion adsorption behavior to Fh is the scaling of ion adsorption data to the surface area of Fh. The primary data refer to the molar ion/Fe ratios that can be translated to adsorption per unit mass and unit surface area, for which the values of molar mass (M_{nano}) and specific surface area (SSA) of Fh are needed. A consistent scaling of ion adsorption data allows the comparison of experimental results obtained for different Fh preparations. For this purpose, consistent assessment of the actual specific surface area (SSA) of Fh is required, as this property is highly variable among different Fh preparations[27,31] and changes over time.[32]

In the presently applied methodology to assess the SSA, the particle size dependency of the molar mass, mass density, and double-layer capacitance of Fh will be considered in an internally consistent manner.[27] This approach enables the development of an internally consistent thermodynamic database with intrinsic ion affinity constants that can be generally used for SCM applications. Our methodology of measuring the SSA differs from traditional analytical techniques for well-crystallized Fe (hydr)oxides because these are not suitable for Fh suspensions kept in the wet state. For instance, N_2 adsorption analysis using the Brunauer−Emmett−Teller (BET) equation requires sample drying and outgassing,[21,33,34] leading to irreversible particle aggregation and lower values of SSA compared to the values found by transition electron microscopy (TEM) measurements.[35] The BET surface area can be 50% lower than the SSA according to TEM,[27] while a similar reduction is also found when comparing the BET surface area with the SSA derived from interpretation of the primary surface charge of Fh with SCM.[27] To overcome this limitation, we have adopted in this study a recently developed systematic approach for assessing the SSA of Fh in which PO_4 serves as a probe ion.[27]

Finally, ion adsorption modeling can be improved using interfacial charge distribution coefficients that have been derived independently with a bond valence analysis[36,37] of the optimized geometry of the formed surface complexes with molecular orbital (MO) calculations using the density function theory (DFT). Such an SCM approach has been successfully applied previously to the modeling of the adsorption of ions to Fh comprising protons and electrolyte ion pairs (Cl^-, ClO_4^-, NO_3^-);[27] PO_4^{3-} and AsO_4^{3-};[26] CO_3^{2-};[38] $H_4SiO_4^0$ and $As(OH)_3^0$;[39] as well as Ca^{2+} and Mg^{2+} ions and their ternary complexes with PO_4^{3-}.[40,41]

In the present study, we will measure the boron adsorption for freshly prepared Fh. Using the above SCM approach, we intend to derive a set of adsorption reactions that can accurately describe our adsorption data in agreement with realistic B surface species that have previously been identified by spectroscopy.[13,16,17,42,43] In addition, we will use the same approach to describe other experimental data reported in the literature[15−17] by consistently accounting for differences in the specific surface area of Fh in these studies. In this approach, the B adsorption behavior will be measured and described for monocomponent systems with Fh. However, one may expect a different B adsorption behavior in natural systems in which omnipresent and strongly adsorbing ions such as phosphate compete with the relatively weakly bound boron. To assess these competition effects, we will also measure the B adsorption to Fh in systems with increasing concentrations of added phosphate.

The final goal of our study is to gain insights into the B speciation in natural systems, and in the relative contribution of Fh in particular, using a multicomponent and multisurface modeling approach. Therefore, we will evaluate with that approach the pH-dependent B adsorption behavior for model systems containing, in addition to Fh, crystalline Fe oxide (goethite) and natural organic matter. For the latter two materials, we will rely on a generic set of model parameters derived previously.[14,44] In the multisurface approach, we will evaluate the importance of PO_4^{3-} and Ca^{2+} ions that are omnipresent in natural soils and interact with the Fe (hydr)oxide surfaces simultaneously with B.

MATERIALS AND METHODS

Fh Synthesis. Fh suspensions were made by adding 0.02 M NaOH to a solution of ∼3.7 mM $Fe(NO_3)_3$ dissolved in 0.01 M HNO_3 as previously described.[27] Initially, the NaOH was added in steps of 100 mL until a pH of ∼3.2 was reached. Subsequently, the NaOH was added in steps of 5 mL until a final pH of 6.0 was reached (pH stable for 15 min). The suspension was left for 4 h to let the particles settle down. Afterward, the suspension was centrifuged for 45 min at 3500*g*. The supernatant was removed, and the Fh particles were collected and resuspended in a background solution of 0.01 M $NaNO_3$ to final volumes of 300 and 225 mL for the suspensions used in the monocomponent and competition systems, respectively.

To reduce possible interference of atmospheric $CO_2(g)$ in the adsorption experiments, the stock Fh suspensions were left overnight and purged under moist $N_2(g)$ until the final aging time of 24 h. For each prepared Fh suspension, we measured the total Fe content in a matrix of 0.8 M H_2SO_4, using inductively coupled plasma-optical emission spectrometry (ICP-OES). The total Fe content was on average 20.5 ± 0.8 mM.

The specific surface area of Fh depends much on the preparation protocol.[32] Since the surface area is an important parameter for consistently scaling and modeling ion adsorption data, we determined the specific surface area independently for each Fh preparation using PO_4 as a probe ion. This approach is a good alternative to overcome the limitations of the BET method,[27] as discussed in the Introduction. Our method has been applied previously to adsorption studies with Fh[38] and described in detail by Mendez and Hiemstra.[27] In this approach, the PO_4 adsorption data are interpreted with the parametrized CD model for Fh[26] and the specific surface area is defined as the only adjustable parameter. In the data treatment, the primary data (molar PO_4/Fe ratios) are scaled to an adsorption per unit mass (mol g^{-1}) and surface area (mol m^{-2}), using the particle-size-dependent molar mass (M_{nano} in g Fh mol^{-1} Fe) and mass density (ρ_{nano} in g m^{-3}) calculated with a consistent set of mathematical relationships.[27,32] The yet unknown surface area is then derived iteratively by CD modeling.

The specific surface area of the Fh preparations used for studying the monocomponent B adsorption was typically in the range A_{PO_4} = 665−677 m^2 g^{-1}, being similar to values found previously.[27] The molar masses corresponding to these SSA values are 96.15−96.45 g mol^{-1} Fe. For the Fh used in the multicomponent B and P adsorption experiment, the specific

https://dx.doi.org/10.1021/acsearthspacechem.0c00078
ACS Earth Space Chem. 2020, 4, 1269−1280

surface area was slightly lower, being A_{PO_4} = 628 m^2 g^{-1} with a molar mass of 95.22 g mol^{-1} Fe.

Boron Adsorption to Fh in Monocomponent Systems. The interaction between B and Fh was assessed by collecting pH-dependent adsorption data in systems with four different total B concentrations (0.05, 0.1, 0.25, 0.4 mM), one concentration of Fh (~8 mM Fe), and a constant ionic strength (0.01 M $NaNO_3$). All systems were made with a total volume of 40 mL.

First, an appropriate volume of 0.01 M $NaNO_3$ was added to a 50 mL polypropylene tube. Next, 16 mL of Fh stock suspension in 0.01 M $NaNO_3$ was pipetted into the tube and the pH was adjusted by adding predetermined amounts of 0.01 M HNO_3 or NaOH. Finally, 2 mL of a freshly prepared $B(OH)_3$ stock solution was pipetted into the tubes.

The pH was adjusted to values between 4 and 11. Systems with pH values lower than pH 4 were avoided to prevent dissolution of the Fh particles. The adsorption systems were equilibrated for 21 h in a horizontal shaker (125 oscillations min^{-1}) at a constant temperature of 20 °C. After equilibration, the samples were centrifuged for 20 min at 3500*g*, and a subsample was subsequently filtered through a membrane filter (0.45 μm). An aliquot of 10 mL was taken and acidified with HNO_3 for B measurement by ICP-OES. The equilibrium pH was measured in the leftover suspension, and this pH value was used as input for the model calculations. An overview of the B adsorption experiments with four different total B concentrations is given in Table S1 (Supporting Information, SI).

Competitive Adsorption of Boron and Phosphate to Fh. The competitive effect of phosphate on B adsorption to Fh was assessed by measuring the adsorption at a fixed pH in a 0.010 M $NaNO_3$ system with a constant amount of added B and Fh but with increasing levels of total added phosphate (0−1.0 mM). For designing the competitive adsorption experiment, preliminary modeling was done using provisional adsorption parameters calculated based on the data from the monocomponent adsorption experiment. This modeling exercise showed that it is difficult to assess accurately the amount of adsorbed B with the traditional method of determining the adsorption from the difference between the initial and the final equilibrium ion concentration because in the presence of PO_4, most of the added B remains in solution due to its relatively low binding affinity. Therefore, we modified our methodology to allow a direct measurement of the amount of B adsorbed by the solid phase.

Our adsorption systems were prepared in 50 mL polypropylene tubes by adding variable volumes of 0.010 M $NaNO_3$ and 16 mL of Fh stock suspension—prepared in 0.01 M $NaNO_3$—followed by adjustment of the pH to 7 using a 0.010 M solution of either NaOH or HNO_3. Subsequently, 2 mL of a 1 mM $B(OH)_3$ stock solution was added together with variable volumes (0−5 mL) of a 0.008 M stock solution of NaH_2PO_4. The pH was checked and adjusted after 3, 5, and 7 h of equilibration. Finally, the total volume was increased to 40.0 mL with 0.01 M $NaNO_3$, and the total equilibration time was set at 21 h. One hour before the end of the experiment, so after 20 h of shaking, the pH was rechecked and adjusted if needed. The corresponding maximum change in volume was 1% or less. The total equilibration time chosen for this study is similar to the time used in previous competitive adsorption experiments with ferrihydrite.[39,41,45]

For the above competitive adsorption experiments, two consecutive centrifugation steps were used in the sampling methodology. After the first centrifugation at 3500*g* for 20 min, most of the supernatant was removed and used for chemical analysis of B, P, and Fe with ICP-OES. In the second step, ultracentrifugation was applied (14 300*g* for 5 min) to maximize the removal of the solution phase from the Fh pellet. With a dispensable pipet, most of the remaining liquid could be removed carefully, and the mass of the remaining paste was measured gravimetrically, showing an average mass of 0.58 g left. Next, the Fh pellet was dissolved by adding 7 mL of 0.8 M H_2SO_4. This extract was measured for B, P, and Fe with ICP-OES.

For calculation of the B adsorption, the B concentration measured in the 0.8 M H_2SO_4 extract was corrected for boron present in the solution left in the Fh paste. The latter can be calculated from the mass of the wet paste (~0.58 g), the mass of the originally added Fh (~0.030 g), and the equilibrium concentration measured in the supernatant collected after the first centrifugation. The adsorbed amount was finally recalculated to the percentage of initially added B in the 40 mL suspension. An overview of the specific experimental conditions of the competitive experiment can be found in Table S1. Since P in the equilibrated solution was extremely low, the PO_4 adsorption is directly found from the P measured after dissolving the Fh paste and scaled to the experimental concentration of Fe measured in the sulfuric acid solution. We modeled adsorbed PO_4 for the specific conditions using parameters from Hiemstra and Zhao,[26] and by comparing it with the experimental PO_4 data, we validated the used approach for measuring the adsorbed P directly.

Modeling Adsorption Data. The adsorption of boric acid to Fh has been modeled using the CD model[25] in combination with the extended Stern layer approach[46] to describe the compact part of the electrical double layer (EDL). A multisite ion adsorption approach was used, as developed recently for Fh.[26] This structural model defines two types of singly coordinated surface groups and a set of triply coordinated groups. The triply coordinated groups present at the Fh surface vary largely in their proton affinity, which leads to an internal charge compensation,[26] making the effective site density for these surface groups smaller. By assuming the same proton affinity for the triply coordinated surface groups as determined for the singly coordinated groups ($\log K$ = 8.1),[26] an effective site density of N_s = 1.4 nm^{-2} was found by fitting phosphate adsorption data.[26] The triply coordinated groups are assumed to be only involved in the development of surface charge and interactions with ions through outer-sphere complexation. Similarly as for proton adsorption, the binding affinity of these groups for (electrolyte) ions is assumed to be the same as for the singly coordinated groups.[26]

With respect to bidentate complex formation, only a fraction of the singly coordinated groups (N_s = 2.8 nm^{-2}) is able to form binuclear complexes (double-corner complexes). Formation of monodentate surface complexes is possible with both types of singly coordinated surface groups (N_s = 5.8 nm^{-2}). The primary surface charge was described with the parameter set presented in the publication by Hiemstra and Zhao[26] and given in Table S2 (SI). The parameters to describe phosphate adsorption were taken from the same study. This parameter set is consistent with the adsorption behavior of Fh measured with the probe ion method using either protons or phosphate.[27]

https://dx.doi.org/10.1021/acsearthspacechem.0c00078
ACS Earth Space Chem. 2020, 4, 1269−1280

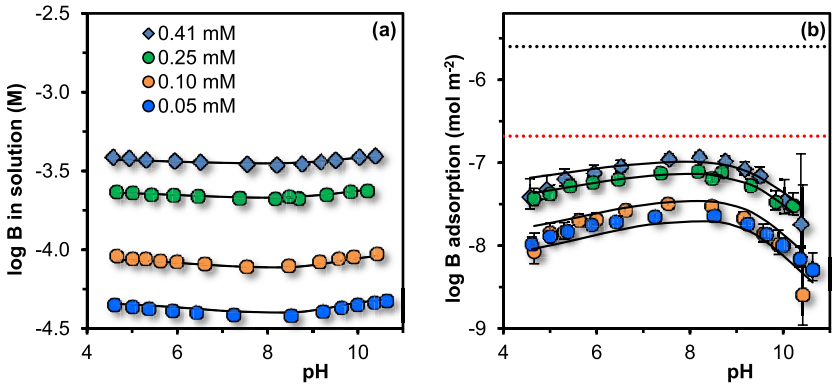

Figure 1. Logarithm of the equilibrium concentration (a) and adsorption (b) of B to Fh as a function of pH in a background solution of 0.01 M $NaNO_3$ at four different total B concentrations. Solid lines represent the modeling results assuming adsorption to singly coordinated groups Fe(OH)(bh) with a high affinity, having a fitted surface density of 0.25 ± 0.08 nm^{-2}. The corresponding maximum adsorption of boron to these sites as a bidentate complex is given as the red dotted line in (b). The black dotted line represents the theoretical maximum adsorption density if the low-affinity sites would contribute to the B adsorption too. Our collected adsorption data are typically within the experimental window with high-affinity sites, which implies that binding to the low-affinity sites cannot be resolved by analysis of our adsorption data with SCM (Table 1). See the discussion in the text. The error bars in (b) represent the variation in adsorbed B when assuming an uncertainty of only 2% in the measured B concentration in solution. The specific experimental conditions can be found in Table S1 (Supporting Information).

As mentioned, Fh is a nanoparticle with a strong surface curvature, which implies that the capacitance values of the Stern layers (C_1 and C_2) are size-dependent, for which we consistently account[47] using the capacitance values for a flat surface as the reference, i.e., C_1 = 0.90 F m^{-2} and C_2 = 0.74 F m^{-2}. Modeling and parameter optimizations were done using the ECOSAT program, version 4.9,[48] in combination with FIT, version 2.581.[49] Input variables were pH, electrolyte ion concentrations, and the total $B(OH)_3$ and PO_4 concentrations, as well as the concentration of Fh (based on the measured Fe content) and its specific surface area (based on the experiments using PO_4 as probe ion). The aqueous B speciation reactions applied in the modeling are given in Table S3 (SI). The only fitted parameters were the log K values, since CD values were calculated based on a Brown valence analysis of the surface species geometry obtained with MO/DFT optimization, as explained by Goli et al.[14]

Multicomponent Model Applications. The B speciation in soils consisting of multiple types of reactive surfaces has been evaluated with a multisurface modeling approach. As crystalline Fe (hydr)oxides may also contribute to the adsorption of B, we considered goethite as a representative crystalline Fe (hydr)-oxide in the assessment of the difference in reactivity relative to nanocrystalline Fh. For boron adsorption to goethite, the parameter set from Goli et al.[14] was used for calculations with the CD-multisite ion complexation (MUSIC) model. The parameters for H^+, PO_4^{3-}, Na^+, and NO_3^- were taken from Hiemstra et al.[50] Boron may also bind to soil organic matter.[10−13] Therefore, its possible contribution to B adsorption has been evaluated using humic acids (HAs) as a model compound for which generic modeling parameters for B have been derived recently.[44]

In our simulations, the chosen amounts of reactive Fe (hydr)oxides and organic matter are representative for Dutch topsoils as reported previously.[50] From the soil data reported by Hiemstra et al.,[50] we chose three contrasting soils that have low and high amounts of organic matter and phosphate. The soil characteristics are given in Table S6 in the Supporting Information. The amount of nanocrystalline oxide, represented by Fh in the modeling, was calculated based on the amount of Fe and Al measured in ammonium oxalate (AO) extracts. The goethite concentration was calculated from the excess amount of Fe found by extraction with dithionite, i.e., $Fe_{dithionite} - Fe_{AO}$. Provisionally, the specific surface area of Fh was taken as 600 m^2 g^{-1} and 100 m^2 g^{-1} for goethite.[51,52] For calculating the equivalent amount of Fh, molar masses of 94 and 84 g mol^{-1} Fe and Al were used, typical for particles with an SSA of 600 m^2 g^{-1},[26] and for goethite, we used 89 g mol^{-1} Fe. Soil organic matter was represented by humic acid assuming that 30% of the total organic matter is reactive and has a carbon content of 50%.[53]

In our modeling, 0.01 M $CaCl_2$ solution was used as a proxy for the soil solution, similar to previous studies that validated a multisurface model for ion partitioning.[52,54,55] The equilibrium concentration of B in the solution phase was set at 1 μM, which is the average concentration that was found for 100 Dutch soils in 0.01 M $CaCl_2$ by Novozamsky et al.[56] Parameters for Ca^{2+} adsorption to humic acids were used from Milne et al.,[57] together with the structural parameters for the site density and the Donnan phase. The Ca^{2+} adsorption parameters for goethite were taken from Hiemstra et al.[50] and for ferrihydrite from Mendez and Hiemstra.[41] In our modeling, we used a linear additivity approach as commonly done in multisurface SCM applications to soils,[51,53,58] which considers distinct individual contributions of the different reactive surfaces to the total ion adsorption. Following this approach, we did not assume either competitive adsorption of organic matter to the Fe (hydr)oxide surfaces or ion complexation with dissolved organic matter.

RESULTS AND DISCUSSION

pH Dependency of B Adsorption to Fh in Mono-component Systems. For Fh, the measured pH-dependent boron adsorption envelopes are given in Figure 1. From the relatively low values for the B adsorption in Figure 1b, it is obvious that the pH-dependent B adsorption is rather weak. The adsorption behavior of B shows a bell-shaped curve with a maximum adsorption around pH 8−9, which is typical for B adsorption to metal oxides.[14,15,42]

The pH dependency of B adsorption is determined by the solution speciation of boron and the interaction of the adsorbing species with protons at the surface, as follows from the thermodynamic consistency equation[39,46,59,60]

https://dx.doi.org/10.1021/acsearthspacechem.0c00078
ACS Earth Space Chem. 2020, 4, 1269−1280

$$(\chi_H - n_H)_{pH} = \left(\frac{\delta \log[B_T]}{\delta(pH)}\right)_{\Gamma_B} \quad (1)$$

This equation shows that the pH dependency of the total solution concentration of boron $[B_T]$ at a constant B loading (Γ_B), given on the right-hand side of the equation, depends on (a) the molar ratio of excess proton coadsorption upon B adsorption (χ_H) and (b) the solution speciation presented by n_H, which is the excess number of protons bound to dissolved boron relative to a chosen reference species, for instance, $B(OH)_3(aq)$.

Model calculations show that the proton coadsorption at acidic pH conditions is around $\chi_H \sim -0.1$. At sufficiently low pH, when $B(OH)_3^0$ is the predominant solution species, the value of n_H approaches zero, which implies that $\chi_H - n_H$ will be negative, so will be the term on the right-hand side of eq 1. Consequently, the change in the equilibrium B concentration with pH will be negative, which agrees with the negative slope at the low pH range for the relationship between the logarithm of the boron concentration in solution and the pH, as shown in Figure 1a. When $B(OH)_4^-$ dominates the solution speciation of B at high pH values (i.e., pH > ~9), $\chi_H - n_H$ becomes larger than 0 due to the negative value of n_H approaching −1 at high pH. In that case, the solution concentration of B will increase with pH, as is found in Figure 1a. Our thermodynamic analysis demonstrates that the bell shape of the adsorption envelope is predominantly due to a change of the B solution speciation. The pH dependency of the B adsorption by Fh has large similarities with the pH-dependent silicate adsorption to Fh that has been discussed by Hiemstra.[39]

The proton coadsorption value that we obtained for Fh is similar to the value obtained when using goethite to calculate the proton coadsorption with parameters from Goli et al.[14] This finding implies that for both Fe (hydr)oxides, the adsorption of B has a similar pH dependency and suggests the existence of similar types of adsorption complexes. This mechanistic interpretation of B adsorption on Fh and goethite will be further elaborated in Comparing B Adsorption to Fh and Goethite.

PO_4-Dependent B Adsorption in Multicomponent Systems. Figure 2 shows the adsorption of PO_4 and B at pH 7.06 ± 0.10 for Fh systems with increasing levels of total added PO_4 and a constant total B concentration. The adsorbed B and PO_4 shown in Figure 2 are based on a direct measurement of the adsorbed quantities after dissolution in 0.8 M H_2SO_4 of the solid phase (i.e., Fh paste; see Materials and Methods). Increase in PO_4 adsorption (orange spheres) significantly reduces the B adsorption in the system (green diamonds). By modeling the adsorption of PO_4 under the same chemical conditions but in the absence of B, we calculated the same PO_4 adsorption as measured in our experiment with B. The presence of B has no significant effect on PO_4 adsorption, since both oxyanions have a very large difference in affinity. At the highest P content (~1 mM), our data reveal that only 5% of the total B is still adsorbed to Fh, compared to 13% in the absence of phosphate.

Based on the results of Figure 2, it can be expected that the B adsorption to nanocrystalline Fe (hydr)oxides will be limited in natural systems since these often contain substantial amounts of adsorbed phosphate. This strong competition of phosphate will reduce the contribution of Fe (hydr)oxides, including Fh, to the surface speciation of B in soils. Consequently, organic matter may become relatively more important for controlling B speciation in soils. This will be further evaluated and discussed in Surface Speciation of B in Soil Systems.

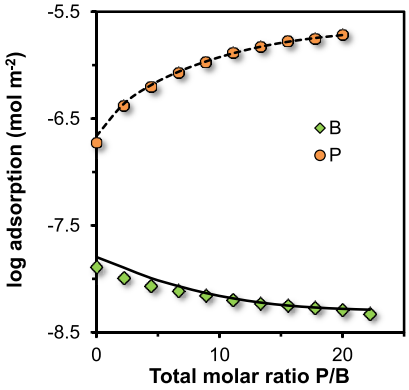

Figure 2. Logarithm of B and PO_4 adsorption as a function of the molar ratio of total P and B in a multicomponent Fh system at pH 7.06 ± 0.10 in 0.01 M $NaNO_3$. The total B concentration was kept constant, but increasing levels of P were added, which leads to an increase in PO_4 adsorption, while the B adsorption decreases due to removal by adsorbed PO_4. The total B concentration was 0.05 mM, the total Fe concentration was 7.88 mM, and the specific surface area of Fh was A_{PO_4} = 628 $m^2\ g^{-1}$. The solid line is the prediction of the B adsorption to the high-affinity sites with a site density of 0.25 ± 0.08 nm^{-2} (Table 1, option B). The dashed line has been calculated using the parameters from Hiemstra and Zhao.[26] According to CD modeling, the PO_4 adsorption is not affected by the presence of boron in the system, which is due to the high intrinsic affinity of phosphate over that of boron.

Modeling B Adsorption Data. *B Surface Complex Formation.* Boron speciation on oxide surfaces has been studied previously at the microscopic scale using different spectroscopic techniques, such as infrared[16,17,42] and X-ray absorption spectroscopy,[61] as well as NMR analysis.[13,43] Using attenuated total reflection-Fourier transform infrared (ATR-FTIR), Su and Suarez[16] found both trigonal and tetrahedral coordination for B with an increasing importance of the tetrahedral species at higher pH values. With ATR-FTIR, Peak et al.[17] assigned two peaks (1330 and 1250 cm^{-1}) to the presence of a trigonal inner-sphere surface species, while a third peak at 1395 cm^{-1} was assigned to an additional trigonal species with similar symmetry to the aqueous boric acid, which was interpreted as an outer-sphere complex. This latter peak was only found at near-neutral pH but not at high pH (~10). Formation of outer-sphere complexes for B has also been identified for manganese oxide,[42] silica gel, and illite.[43] With the above spectroscopic information, no distinction can be made between the presence of monodentate or bidentate surface species of B. However, based on isotopic fractionation, Lemarchand et al.[42] concluded that boron binds likely as a bidentate complex to the goethite surface.

Based on the above, we formulated for Fh two inner-sphere bidentate complexation reactions with the formation of a trigonal (eq 2) and tetragonal (eq 3) surface species

$$2{\equiv}FeOH(b)^{-0.5} + B(OH)_3(aq) \leftrightarrow {\equiv}(FeO)_2B(OH) + 2H_2O\ (l) \quad (2)$$

$$2{\equiv}FeOH(b)^{-0.5} + B(OH)_3(aq) \leftrightarrow {\equiv}(FeO)_2B(OH)_2 + 1H_2O(l) + H^+(aq) \quad (3)$$

https://dx.doi.org/10.1021/acsearthspacechem.0c00078
ACS Earth Space Chem. 2020, 4, 1269−1280

Table 1. Surface Species of Boron with Fh, Using a Modeling Approach either without (A) or with (B) High-Affinity Sites[a]

species	Δz_o	Δz_1	Δz_2	log K^c	log K^d
$\equiv(FeO(b))_2^{-0.82}B(OH)^{-0.18}$	0.18[b]	−0.18[b]	0	2.17 ± 0.13	3.39 ± 0.18
$\equiv(FeO(b))_2^{-1.25}B(OH)_2^{-0.75}$	−0.25[b]	−0.75[b]	0	−5.85 ± 0.08	−4.68 ± 0.20
$\equiv Fe_3OH^{0.5}\cdots B(OH)_3^0$	1	0	0	9.33 ± 0.08	9.32 ± 0.07
$\equiv FeOH_2(a)^{0.5}\cdots B(OH)_3^0$	1	0	0	9.33 ± 0.08	9.32 ± 0.07
$\equiv FeOH_2(b)^{0.5}\cdots B(OH)_3^0$	1	0	0	9.33 ± 0.08	9.32 ± 0.07

[a]The interfacial CD values (Δz_o and Δz_1) are from Goli et al.[14] The applied extended Stern layer model uses two capacitance values consistent with the specific surface area of Fh given in Table S1. The surface reactions defining the primary charge are given in Table S2. The values for log K are taken as the average and standard deviation of the fitted values using two evaluation scales (i.e., % B adsorbed and log mol m^{-2} B adsorbed). Fitted values, R^2, and root-mean-square error (RMSE) for each evaluation scale are given in Tables S4 and S5 (SI). Site densities of $\equiv Fe_3O$, $\equiv$FeOH(a), and $\equiv$FeOH(b) were taken as 1.4, 3.0, and 2.8 sites nm^{-2} for scenario A.[26] For scenario B, the inner-sphere complexes are only formed with high-affinity sites that are a subtype of the $\equiv$FeOH(b) surface groups with a fitted site density of 0.25 ± 0.08 sites nm^{-2}. [b]CD values based on MO/DFT calculations of Goli et al.[14] [c]Considering the total set of singly coordinated groups (FeOH(b)) that can form bidentate double-corner complexes, with a site density of 2.8 sites nm^{-2}. [d]Considering only a set of singly coordinated groups that can form bidentate binuclear complexes, with fitted site density of high-affinity sites of 0.25 ± 0.08 sites nm^{-2}.

in which $\equiv FeOH(b)^{-1/2}$ represents the type of singly coordinated surface groups that may form double-corner (^{2}C) bidentate complexes at the surface of Fh. Other singly coordinated groups ($\equiv FeOH(a)^{-1/2}$) may form single-edge (^{1}E) bidentate complexes on the ferrihydrite surface as found for uranyl.[62] From the literature, it is not known whether edge-sharing complexes might be important for B, and we will assume, therefore, only the formation of bidentate corner-sharing complexes. The site density of $\equiv FeOH(b)^{-1/2}$ is 2.8 nm^{-2} according to a structural analysis of the Fh surface.[26]

The above-described multisite model of Fh has also been used previously to describe the adsorption of oxyanions such as PO_4^{3-}, $H_4SiO_4^0$, and CO_3^{2-} to Fh.[26,38,39] More recently, the model has been extended to describe the adsorption of alkaline-earth metal cations.[40,41] Analysis of the adsorption data of this metal cation series shows that the adsorption can only be described over a vast range of surface loadings by distinguishing both high-affinity ($\equiv FeOH(bh)^{-1/2}$) and low-affinity ($\equiv FeOH(bl)^{-1/2}$) sites. In the data analysis below, we will discuss whether this surface site heterogeneity is also important for the binding of boron.

As spectroscopy data also suggests the formation of outer-sphere complexes, the following reactions were formulated for binding of B to singly ($\equiv FeOH^{-1/2}$) and triply ($\equiv Fe_3O^{-1/2}$) coordinated surface groups

$$\equiv FeOH^{-0.5} + H^+(aq) + B(OH)_3(aq) \leftrightarrow \equiv FeOH_2\cdots B(OH)_3 \quad (4)$$

$$\equiv Fe_3O^{-0.5} + H^+(aq) + B(OH)_3(aq) \leftrightarrow \equiv Fe_3OH\cdots B(OH)_3 \quad (5)$$

in which $\equiv FeOH^{-1/2}$ represents the full collection of singly coordinated groups ($FeOH^{-1/2}$(a) and $FeOH^{-1/2}$(b)) with a total site density of N_s = 5.8 nm^{-2} and $\equiv Fe_3O^{-1/2}$ represents the triply coordinated groups with a site density of 1.4 nm^{-2}. The affinity of the singly and triply coordinated groups for B outer-sphere complexation is assumed to be equal, similarly as for the electrolyte ions and for the development of charge on the Fh surface.[26]

For the above bidentate inner-sphere surface species that share corners with Fe(III) octahedra (eqs 2 and 3), Goli et al.[14] optimized the geometry using molecular orbital (MO) calculations applying the density functional theory (DFT). These geometries were used to calculate the CD coefficients by applying a Brown bond valence analysis[63] with a correction for dipole orientation of water molecules.[46] In our study, the values for these CD coefficients were used (Table 1) and only the corresponding log K values of the adsorption reactions were fitted.

Initial Modeling. For our parameter optimization, we used the experimental data from both the B monocomponent systems and the multicomponent system with PO_4. The log K values were derived by evaluating the adsorption data rather than the equilibrium boron concentrations in solution because the variation in the equilibrium solution concentration with pH is smaller than that of adsorbed B (Figure 1). The final log K values were taken as the average of values fitted on the basis of the % adsorbed and of the log of adsorbed B in mol m^{-2}. In the modeling, we used for each Fh preparation the specific surface area that was measured independently with PO_4 surface probing and employed the corresponding size-dependent capacitance values, which were derived by applying the spherical double-layer theory to the compact part of the electrical double layer (EDL).[47]

In a first attempt to model the collected data accurately, it was assumed that all FeOH(b) sites contributed equally to the binding of boron, forming double-corner (^{2}C) bidentate complexes. When using all data points (n = 59) from the mono- and multicomponent systems, formation of inner-sphere and outer-sphere complexes could be revealed. The corresponding log K values for each evaluation scale (i.e., % B adsorbed and log B adsorbed in mol m^{-2}) are given in the Supporting Information (Table S4), together with the quality of the fit (R^2). The model predictions are given in Figures S1 and S2. The use of either evaluation scale resulted in similar log K values for all surface species.

The log K value derived for the formation of outer-sphere complexes by Fh is equal to the log K found for goethite, taking as a reference the positively charged $\equiv FeOH_2^{+1/2}$ group and writing the adsorption reaction as $\equiv FeOH_2^{+1/2} + B(OH)_3(aq) \Leftrightarrow \equiv FeOH_2^{1/2}-B(OH)_3$. The fitted value is log K = 1.24 ± 0.06 for Fh and log K = 1.22 ± 0.21 for goethite. The log K of this outer-sphere complex is significantly higher than found for classical electrolyte ions such as NO_3^- (log K = −0.68), Cl^- (log K = −0.45), and Na^+ (log K = −0.60).[46] This might suggest the formation of a relatively stronger H-bond between $\equiv FeOH_2^{+1/2}$ and the adsorbed $B(OH)_3$ species, which might affect the assumed charge distribution. We have tried to optimize the geometry of a cluster representing the hydrated $\equiv FeOH_2^{1/2}-B(OH)_3$ surface species with MO/DFT calculations,

https://dx.doi.org/10.1021/acsearthspacechem.0c00078
ACS Earth Space Chem. 2020, 4, 1269−1280

using the B3LYP model in Spartan'14 parallel software of Wavefunction. In the optimization, the boric acid was initially attached to the $\equiv FeOH_2^{+1/2}$ group with a strong H-bond. However, the hydrated $B(OH)_3$ species drifted away, suggesting that no extra shift of proton charge (i.e., relative to our originally assumed charge distribution of $\Delta z_0 = +1$ v.u. and $\Delta z_1 = 0$ v.u.) is expected in the interface upon interaction of B in an outer-sphere manner. Based on this result, we conclude that the original CD values from Table 1 used in the formation reaction of the outer-sphere complexes can be considered as reasonable.

In a recent study,[39] it has been shown that silicic acid, $Si(OH)_4(aq)$, may bind to Fh as a monodentate complex that reacts with an adjacent singly coordinated surface group, forming a strong H-bond ($\equiv FeHO\cdots H-OSi$). To explore this possibility for boric acid, we performed several MO/DFT/B3LYP calculations, searching for the formation of a strong H-bond if a monodentate $\equiv FeOB(OH)_2$ complex interacts with an adjacent singly coordinate group, being either $\equiv FeOH_2^{+1/2}$ or $\equiv FeOH^{-1/2}$. The optimizations show that the B−OH ligand does not form a strong H-bond with the adjacent surface group, i.e., its formation is less likely than the formation of a classical bidentate complex $\equiv(FeO)_2BOH$ with the CD as calculated (Table 1).

Our initial modeling attempt showed a systematically larger concentration dependency of the B adsorption than observed experimentally (Figure S2). At low B concentrations, the adsorption was underestimated by the model, and at high concentrations, it was overestimated. The experimental data suggest a less linear adsorption behavior than suggested by the model. When the adsorption data (Q) are fitted to a Freundlich model, $Q = K_F c^n$, the coefficient n for the concentration dependency is $n = 0.77$ (Figure 3). With the predicted

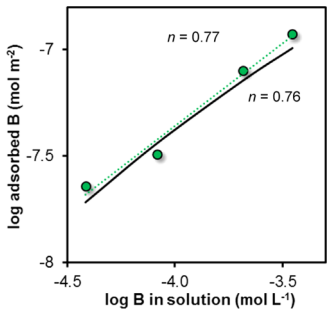

Figure 3. Adsorption isotherm for boron binding to Fh at pH 8.0 in 0.01 M $NaNO_3$. The data points (green symbols) were derived by interpolation of the pH-dependent B adsorption data from Figure 1. The full line is the CD modeling result, considering bidentate inner-sphere complex formation by reaction of B with high-affinity sites having a site density of 0.25 ± 0.08 sites nm^{-2}. The CD model parameters are given in Table 1, option B. The dotted green line is the Freundlich adsorption isotherm ($\log Q = \log K_F + n \log C$) with a fitted slope of $n = 0.77$ in a double logarithmic plot that is close to the mean slope ($n = 0.76$) predicted by the CD model.

adsorption using the initial model option (Table 1, option A), it is equivalent to $n = 0.91$ (not shown), which means that the model in that case predicts a more linear adsorption behavior than shown by the experimental data. As pointed out by Benjamin and Leckie,[64] deviation from linear adsorption behavior ($n = 1$) can be caused by the existence of multiple types of binding sites with different affinities if not due to ignoring electrostatic energy contributions. The presence of high- and low-affinity sites has been used frequently in modeling surface complexation of ions by ferrihydrite, particularly for metal cations.[21,41,45,65,66]

Introducing High-Affinity Sites. Based on the above, we have explored the possible role of the presence of a limited number of surface sites with a higher affinity for binding B, forming inner-sphere bidentate surface complexes. In this modeling option, the $\equiv FeOH(b)^{-1/2}$ sites were initially divided into two classes, each class with a different intrinsic affinity ($\log K$) for boron. The site densities were fitted with the restriction that the sum of the densities of $\equiv FeOH(bh)^{-1/2}$ and $\equiv FeOH(bl)^{-1/2}$ equals the overall density of $\equiv FeOH(b)^{-1/2}$. Formation of outer-sphere complexes was considered as explained before. No $\log K$ value for B binding to the low-affinity sites ($\equiv FeOH(bl)^{-1/2}$) could be found by fitting under these boundary conditions, and only the set of surface groups with higher affinity ($\equiv FeOH(bh)^{-1/2}$) played a role in B binding. With this approach, the quality of our data description substantially improved (Figure 1 vs Figure S1 and S2). Also important was the outcome of the fitted value for the site density of the high-affinity sites, being $N_s(bh) = 0.25 \pm 0.08$ nm^{-2}. This value is very similar to the value that has been found recently for the adsorption of alkaline-earth metal ions (Ca^{2+}, Sr^{2+}), also forming double-corner bidentate complexes with singly coordinated surface groups,[40] being on the order of $N_s(bh) = 0.30 \pm 0.02$ nm^{-2}.

Mendez and Hiemstra[40] identified a possible structural feature at the surface of Fh that might explain the observed surface density of the high-affinity sites and, in addition, gives a rationale for the high-affinity character of the singly coordinated groups of those sites. It is suggested that for the pair of Fe(III) octahedra involved in the high-affinity sites, the oxygen charge of the ligands common to the mineral bulk is collectively slightly undersaturated, resulting in some redistribution of charge within this moiety, making both singly coordinated groups of this unit more reactive, thus increasing their affinity for an adsorbing ion. Per particle, about three pairs of such $\equiv FeOH(bh)$ sites could be found when Fh particles were constructed according to the surface depletion model.[29] For our Fh suspensions, this number is equivalent to a site density of about 0.3 nm^{-2}, which is consistent with the number found here by fitting the $B(OH)_3$ adsorption data (0.25 ± 0.08 nm^{-2}).

A major difference with the alkaline-earth metal ion adsorption is that for boron, no binding to low-affinity sites ($\equiv FeOH(bl)^{-1/2}$) could be established, while for the metal cations of the alkaline-earth series, this is clearly found. To understand this difference, we plotted the maximum possible $B(OH)_3$ adsorption in the case of only binding to high-affinity sites (red dotted line in Figure 1b). This representation indicates that our experimental surface B loadings are significantly lower. The affinity of boron is too low to saturate these sites to a sufficient level at which additional adsorption to low-affinity sites starts to occur. For this reason, binding to low-affinity sites cannot be resolved with our present data set. This contrasts with the adsorption of metal ions that may adsorb to Fh over a larger range of surface loadings.[40]

In the literature, the presence of high-affinity sites has been particularly associated with the binding of cations, but this concept has not been applied so far to the modeling of the adsorption data of oxyanions. One plausible explanation for this difference might be that oxyanions such as PO_4 and AsO_4 are bound strongly to ferrihydrite, which does not enable identification of the relatively small number of high-affinity sites. Another possibility can be that the anion adsorption is

https://dx.doi.org/10.1021/acsearthspacechem.0c00078
ACS Earth Space Chem. 2020, 4, 1269−1280

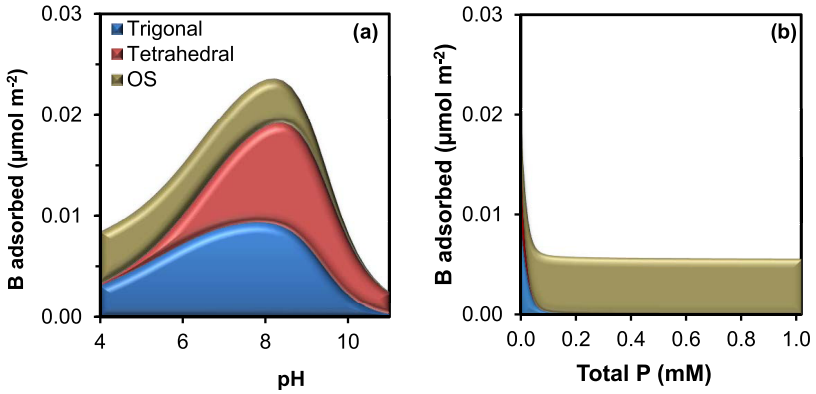

Figure 4. Surface speciation of B calculated in relation to pH (a) and to total P (b) in the Fh system. Boron can be bound to Fh as a trigonal or a tetrahedral inner-sphere bidentate complex or as an outer-sphere (OS) species. Model calculations were done using the CD model (Table 1) with high-affinity sites for the B adsorption. Parameters for the PO_4 adsorption were taken from Hiemstra and Zhao.[26] The total B concentration was 0.05 mM with an Fh concentration of 0.8 g L^{-1}. The used surface area of Fh was A = 668 m^2 g^{-1}. The background electrolyte was 0.01 M $NaNO_3$. In (b), the pH was fixed at 7.

dominated by the formation of other types of surface complexes such as outer-sphere complexes, inner-sphere monodentate complexes, or bidentate edge complexes, which do not bind to high-affinity sites.

With the introduction of high-affinity sites for the adsorption of boron, a significantly smaller concentration dependency is predicted by the model compared to the initial modeling option that considers the binding of B to all FeOH(b) sites. When the adsorption isotherm is presented in a double log plot (Figure 3), the slope from the modeling predictions based on high-affinity sites (Table 1, option B) is n = 0.76, which is much closer to the fitted slope of the data (n = 0.77) than when using the complete set of sites for B binding (Table 1, option A, n = 0.91). This analysis underlines the improvement of the data description when considering binding of boron only to a limited number of surface sites with a high-affinity character.

In a study of B adsorption to amorphous Al oxide, Xu and Peak[61] found a significant reduction of B adsorption due to the presence of carbonate in an open experimental system with continuous input of CO_2. Presently, we have worked with closed systems, but nevertheless, we have assessed the possible effect of CO_2 in our experiments on the fitted log K values. In our analysis, we assumed that the aqueous solutions used to prepare our closed systems were initially in equilibrium with CO_2 at an atmospheric partial pressure of 0.4 mbar (i.e., ~20 μM CO_3^{-2}, pH ~5.6). With CD model calculations using the parameters from Mendez and Hiemstra,[38] we did not find any significant effect of the presence of dissolved CO_2 on B adsorption. The same has been concluded by Goli et al.[14] for B adsorption to goethite in closed systems.

We evaluated our parameters for B adsorption to Fh for other experimental data reported in the literature, using the specific surface area of Fh as an adjustable parameter.[15−17] The results are shown and discussed in the Supporting Information (Figures S3 and S4). The B adsorption at low pH was underestimated for the experimental data from Goldberg and Glaubig[15] and Peak et al.,[17] but the experimental data from Su and Suarez[16] were reasonably well described.

Surface Speciation of B. Using the CD model parameters from Table 1 (scenario B, high-affinity sites), we calculated for Fh the B surface speciation as a function of pH (Figure 4a) and as a function of total PO_4 concentration at a constant pH value of 7.0 (Figure 4b). The chosen conditions are representative of our experiments.

In the monocomponent system of Figure 4a, the trigonal inner-sphere complex is the most important surface species below pH ~8. At higher pH, the tetrahedral species becomes more relevant. Outer-sphere complexation is predicted to contribute only at low pH values, while above pH 9, it is practically absent.

In the presence of PO_4, the speciation changes drastically (Figure 4b). The inner-sphere complexation is strongly reduced and becomes negligible at total P concentrations of just 0.1 mM, in contrast to the presence of outer-sphere complexation that remains unaffected by the increasing levels of PO_4 in the system. This difference in surface speciation of B in the absence and presence of PO_4 can be attributed to electrostatic interactions. In general, competition by electrostatic interactions mainly occurs via charge attribution to the Stern plane (Δz_1). Upon adsorption, the inner-sphere complexes of B and P both introduce negative charge to the 1-plane of the Stern layer. Due to the higher affinity of PO_4 for the surface, the B inner-sphere complexes with Δz_1 = −0.18 and −0.75 (Table 1) therefore decrease rapidly when phosphate concentrations increase. On the other hand, $B(OH)_3$ bound as an outer-sphere complex does not introduce in our model any charge in the 1-plane (Δz_1 = 0; see Table 1). Consequently, the formation of this complex is unaffected by electrostatic competition in the 1-plane.

The above conclusion with respect to the relative importance of outer-sphere complexation is supported by our observations during a stepwise modeling approach. When using only the data from the monocomponent systems, no log K value could be derived with certainty for the outer-sphere surface species. In the monocomponent systems (Figure 4a), this species only contributes in the low to neutral pH range, and only in a minor proportion, making it difficult to distinguish this surface species in the fitting procedure from the dominating inner-sphere complex. However, including the data from the competitive adsorption experiment with PO_4 made it possible to derive a log K value for the outer-sphere complex with a relatively low uncertainty (±0.07) because at these conditions the B outer-sphere complex is the dominant species (Figure 4b). This indicates that the inclusion of competitive adsorption experiments in the derivation of binding constants can be helpful

https://dx.doi.org/10.1021/acsearthspacechem.0c00078
ACS Earth Space Chem. 2020, 4, 1269−1280

to identify and increase certainty about specific surface species and the quality of their log K values.

Comparing B Adsorption to Fh and Goethite. Natural systems consist of multiple reactive surfaces, which can adsorb B and consequently affect the B speciation.[10,13,67] Boron may interact with the short-range-order iron oxides of soils (i.e., Fh) as well as crystalline iron oxides (i.e., goethite). Both ferrihydrite and goethite show for boric acid a similar bell-shaped adsorption envelope (Figure 5a) and surface loading. However, the affinity

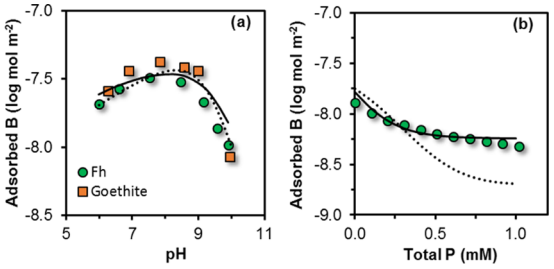

Figure 5. (a) Logarithm of the B adsorption (log mol m^{-2}) as a function of pH. Our data for Fh (circles) refer to a system with 0.1 mM B in 0.01 M $NaNO_3$. The data for goethite (squares) are from Goli et al.[14] and refer to a system with the same B concentration but a slightly higher background electrolyte concentration (0.05 M $NaNO_3$, which does not significantly affect the B adsorption, as shown by these authors). Dotted lines show the modeling results for goethite, using the CD model parameters from Table 2 in Goli et al.,[14] at a concentration of 6 g L^{-1} goethite with a specific surface area of 94 m^2 g^{-1}. Full lines show the modeling results for Fh using the parameters from Table 1 and using high-affinity sites together with a concentration of 0.81 g L^{-1} Fh with a specific surface area of 665 m^2 g^{-1}. (b) Logarithm of B adsorption as a function of the initial P concentration in the Fh system at pH 7 and with 0.05 mM B in 0.01 M $NaNO_3$. The data points for Fh are the same as in Figure 2. The model lines were calculated with 0.80 g L^{-1} and 628 m^2 g^{-1} for Fh (full line) and 5 g L^{-1} and 100 m^2 g^{-1} for goethite (dotted line), to have in both systems the same available surface area (m^2 L^{-1}).

constant of trigonal bidentate species is substantially higher for ferrihydrite. We found log K = 3.4 ± 0.05 for ferrihydrite (Table 1), while for goethite, the value is lower, being log K = 2.6 ± 0.1.[14] This difference in affinity might be due to the difference in the types of reactive sites involved. The difference in affinity does not lead to a higher adsorption, probably because of the much lower reactive site density for B binding to Fh (0.25 ± 0.08 nm^{-2}) compared to that of goethite (3.45 nm^{-2}). For the tetragonal surface species, the log K is also significantly higher for ferrihydrite (log K = −5.3 ± 0.6) than for goethite (log K = −7.7 ± 0.4). This contrasts with the affinity constants for outer-sphere complex formation, which are very similar if we correct for the difference in proton affinity of both materials, as discussed above in Initial Modeling. The observed differences as well as similarities are consistent with the different types of sites involved in B complexation, namely, ordinary (goethite) and high-affinity (Fh) sites.

From Figure 5a, it is evident that Fh and goethite have a similar B adsorption when scaled to the surface area. This finding suggests that in terms of SCM applications to natural systems, the surface area of the metal oxide fraction is a more important parameter than the type of Fe (hydr)oxide used as model oxide material. However, for other oxyanions, both minerals may differ in reactivity, and this may lead to another boron adsorption as the result of a different competitive behavior. If we compare the effect of PO_4 on the B adsorption of goethite and Fh, CD modeling predicts that the presence of PO_4 decreases the B adsorption to goethite more strongly (Figure 5b). Although the log K value for the outer-sphere B surface species for both model oxides is the same, the total site density for the formation of outer-sphere complexes is higher for Fh, resulting in a higher B adsorption to Fh than to goethite at high PO_4 concentrations. This observation underlines that in evaluations of the boron adsorption of soils, differentiation between both types of Fe (hydr)oxides may be relevant for unveiling the surface speciation of B. This will be further discussed in the next section.

Surface Speciation of B in Soil Systems. Besides Fe (hydr)oxides, boron may also bind to natural organic matter.[10,13,44,67] To estimate the relative importance of organic matter for B adsorption, we calculated the binding of B for a system containing organic matter in addition to nanocrystalline and crystalline Fe (hydr)oxide loaded with PO_4. The B binding by natural organic matter has been assessed recently using the NICA–Donnan model.[44] For modeling the adsorption of B to the crystalline Fe (hydr)oxides, we rely on the CD model parameters reported for goethite.[14] For Fh, the modeling results are based on the adsorption parameters obtained in this study, as given in Table 1, option B. Our model simulations were done for

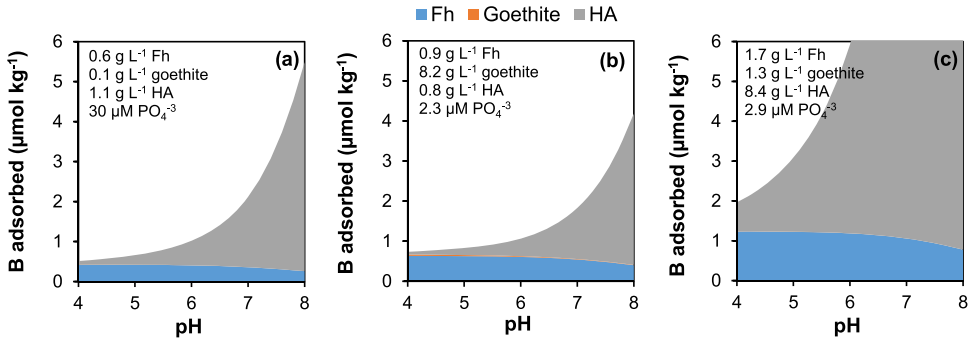

Figure 6. pH-dependent B adsorption expressed in μmol kg^{-1} of soil. Calculations were done for a system containing natural organic matter (HA), nanocrystalline iron-(hydr)oxide (Fh), and crystalline Fe (hydr)oxide (goethite), in a background solution of 0.01 M $CaCl_2$ at a solid-to-solution ratio of 1:10. The modeling scenarios are for systems with a low (a, b) and a high (c) organic matter content having a low (b, c) and a high (a) level of PO_4 in solution. The soil oxide fraction is represented by Fh and goethite having a specific surface area of, respectively, 600 and 100 m^2 g^{-1}. Organic matter (OM) is represented by humic acids. The B concentration in the solution phase is kept constant as 1 μM. For more details about modeling input, we refer to the Supporting Information (Table S6). The B adsorption modeling to Fh was done with parameters from Table 1, using high-affinity sites. The B adsorption parameters for goethite and HA were taken from Goli et al.[14,44]

https://dx.doi.org/10.1021/acsearthspacechem.0c00078
ACS Earth Space Chem. 2020, 4, 1269−1280

three agricultural soils from The Netherlands for which the data regarding reactive surfaces and PO_4 loading were collected in a previous study.[50] The three soils differ in the amount of organic matter, Fe and Al (hydr)oxides, and phosphate loading (Table S6 (SI)). Importantly, our calculations have been done for systems with a (for soil solution more representative) background concentration of 0.01 M $CaCl_2$.

Our modeling shows that the Fe (hydr)oxides dominate the boron binding at low pH. For all three soils, the contribution of goethite to B adsorption is minor. In soils with similar mass fractions of the nanocrystalline and crystalline Fe (hydr)oxide (Figure 5c), the binding is dominated by ferrihydrite because for this oxide, the specific surface area is much higher, and the competitive effect of PO_4 is lower compared to goethite. There is relatively little pH dependency for B binding to the Fe(hydr)-oxides in the subneutral pH range; the typical bell shape of the adsorption envelope observed in the monocomponent oxide systems is lost for these materials due to the presence of PO_4.

For organic matter, the boron envelope remains bell-shaped when extrapolated to higher pH values than shown in Figure 6, as was found before,[44] since it is not affected by the presence of PO_4. Consequently, the boron adsorption may not change importantly in alkaline soils by the addition of PO_4, which was observed by Majidi et al.[68] Because of this difference in pH dependency of B adsorption, the contribution of organic matter becomes increasingly important at increasing pH.

In soils rich in organic matter (Figure 5c), the binding of B to organic matter is predicted to dominate the adsorption in nearly the entire pH range. In soils with less organic matter (Figure 5a,b), the natural metal (hydr)oxide fraction may contribute significantly at low pH in the case of a sufficiently high content of ammonium oxalate extractable Fe and Al (i.e., similar concentration of Fh in terms of mass compared to HA). In soils with a high content of organic matter (Figure 5c), Fh can still contribute to about half of the B adsorption between pH 4 and 5. Our comparison of the B adsorption to the various reactive surfaces provides a mechanistic explanation for the suggestion from Gu and Lowe[11] that in soil systems, oxides may contribute to B binding at a relatively low pH.

CONCLUSIONS

In this study, we evaluated the boron adsorption by ferrihydrite nanoparticles, collecting experimental data and performing state-of-the-art surface complexation modeling. Interestingly, we found that the data could be best described when using a set of singly coordinated groups that act as high-affinity sites for B adsorption to Fh. The adsorption densities that were found in our experimental window are clearly below the saturation level of these high-affinity sites, and as a result, no binding to surface sites with lower affinity could be detected.

The B adsorption data were described using a set of surface species identified previously by spectroscopy. The adsorption at low pH is dominated by the formation of a trigonal bidentate surface species with a contribution of an outer-sphere complex. At high pH, a tetrahedral bidentate complex becomes increasingly important. Our experimental data have shown that PO_4 can strongly reduce the B adsorption on Fh. In the presence of PO_4, the only remaining surface species was found to be an outer-sphere complex because this complex does not introduce charge into the first Stern plane and, therefore, it is little affected by the electrostatic repulsion induced by the adsorption of PO_4.

We found that the pH-dependent B adsorption density of Fh is similar to that of goethite, which was shown both experimentally and by CD modeling. However, modeling showed that the effect of PO_4 on B binding differs between Fh and goethite, with a larger reduction in B binding to goethite due to the presence of PO_4. These findings imply that for natural systems the choice of a reference oxide (i.e., Fh or goethite) for describing the B adsorption is important as competitive ions such as PO_4 are usually present.

The derived adsorption parameters for B binding to Fh are internally consistent with those previously derived for other ions, using a common modeling framework. This work thus contributes to the enlargements of the consistent thermodynamic database for SCM using Fh as the model oxide.

To gain insights into B speciation in soil systems, we assessed the importance of B binding to oxides relative to organic matter, in a multisurface modeling simulation. In the low pH range, the boron adsorption by organic matter is relatively low, and under these conditions, the natural metal (hydr)oxide fraction and especially Fh may significantly contribute to the total boron binding if the oxalate extractable fraction of Fe and Al is sufficiently high (i.e., equal mass of Fh and solid humic acids). Even in soils rich in organic matter, Fh can still contribute to about half of the total B adsorption when the pH is between pH 4 and 5. In the presence of PO_4, the typical bell-shaped pH-dependent B adsorption to oxides is lost, and as a result, the B speciation at high pH is predicted to be controlled by the adsorption to organic matter.

Our new adsorption parameters and state-of-the-art model predictions have important implications for understanding the B availability and mobility in soil systems at different pH values and with variable inputs of phosphate, due to for instance liming and fertilization.

ASSOCIATED CONTENT

Supporting Information

The Supporting Information is available free of charge at https://pubs.acs.org/doi/10.1021/acsearthspacechem.0c00078.

Experimental conditions of the monocomponent and competitive batch adsorption systems (1), thermodynamic database with log K and CD values used in CD modeling (2), aqueous boron species used in CD modeling (3), log K values found by fitting at different scales when using the complete set of sites for complexation with B (4), log K values found by fitting at different scales when using a subset of high-affinity sites for complexation with B (5), soil properties of Dutch soils used for modeling of B speciation in systems with oxides and organic matter (6), modeling calculations when using the complete set of sites for surface complexation with B (7), literature data for B adsorption to ferrihydrite (8) (PDF)

AUTHOR INFORMATION

Corresponding Author

Elise Van Eynde − *Department of Soil Chemistry and Chemical Soil Quality, Wageningen University, 6708 PB Wageningen, The Netherlands;* orcid.org/0000-0002-1106-1541; Email: elise.vaneynde@wur.nl

https://dx.doi.org/10.1021/acsearthspacechem.0c00078
ACS Earth Space Chem. 2020, 4, 1269−1280

Authors

Juan C. Mendez − *Department of Soil Chemistry and Chemical Soil Quality, Wageningen University, 6708 PB Wageningen, The Netherlands;* orcid.org/0000-0002-1658-400X

Tjisse Hiemstra − *Department of Soil Chemistry and Chemical Soil Quality, Wageningen University, 6708 PB Wageningen, The Netherlands*

Rob N. J. Comans − *Department of Soil Chemistry and Chemical Soil Quality, Wageningen University, 6708 PB Wageningen, The Netherlands*

Complete contact information is available at: https://pubs.acs.org/10.1021/acsearthspacechem.0c00078

Author Contributions

The manuscript was written through contributions of all authors. All authors have given approval to the submitted version of the manuscript.

Notes

The authors declare no competing financial interest.

■ ACKNOWLEDGMENTS

This work was supported by NWO (grant number 14688, "Micronutrients for better yields"). All experiments and analyses were done in the CBLB laboratory at Wageningen University and Research. We greatly appreciate the help from Peter Nobels and Wobbe Schuurmans for the ICP-measurements.

■ REFERENCES

(1) Uluisik, I.; Karakaya, H. C.; Koc, A. The Importance of Boron in Biological Systems. *J. Trace Elem. Med. Biol.* **2018**, *45*, 156−162.

(2) Bassett, R. L. L. A Critical Evaluation of the Thermodynamic Data for Boron Ions, Ion Pairs, Complexes, and Polyanions in Aqueous Solution at 298.15 K and 1 Bar. *Geochim. Cosmochim. Acta* **1980**, *44*, 1151−1160.

(3) Kabata-Pendias, A. *Trace Elements in Soils and Plants*, 3rd ed.; CRC Press, 2001.

(4) Shorrocks, V. M. The Occurrence and Correction of Boron Deficiency. *Plant Soil* **1997**, *193*, 121−148.

(5) Howe, P. D. A Review of Boron Effects in the Environment. *Biol. Trace Elem. Res.* **1998**, *66*, 153−166.

(6) Gupta, U. C.; Jame, Y. W.; Campbell, C. A.; Leyshon, A. J.; Nicholaichuk, W. Boron Toxicity and Deficiency: A Review. *Can. J. Soil Sci.* **1985**, *65*, 381−409.

(7) Goldberg, S. Reactions of Boron with Soils. *Plant Soil* **1997**, *193*, 35−48.

(8) Keren, R.; Bingham, F. T.; Rhoades, J. D. Plant Uptake of Boron as Affected by Boron Distribution Between Liquid and Solid Phases in Soil. *Soil Sci. Soc. Am. J.* **1985**, *49*, 297−302.

(9) Kot, F. S. Boron Sources, Speciation and Its Potential Impact on Health. *Rev. Environ. Sci. Bio/Technol.* **2009**, *8*, 3−28.

(10) Goldberg, S. Chemical Modeling of Boron Adsorption by Humic Materials Using the Constant Capacitance Model. *Soil Sci.* **2014**, *179*, 561−567.

(11) Gu, B.; Lowe, L. E. E. Studies on the Adsorption of Boron on Humic Acids. *Can. J. Soil Sci.* **1990**, *70*, 305−311.

(12) Keren, R.; Communar, G. Boron Sorption on Wastewater Dissolved Organic Matter: PH Effect. *Soil Sci. Soc. Am. J.* **2009**, *73*, 2021−2025.

(13) Lemarchand, E.; Schott, J.; Gaillardet, J. Boron Isotopic Fractionation Related to Boron Sorption on Humic Acid and the Structure of Surface Complexes Formed. *Geochim. Cosmochim. Acta* **2005**, *69*, 3519−3533.

(14) Goli, E.; Rahnemaie, R.; Hiemstra, T.; Malakouti, M. J. The Interaction of Boron with Goethite: Experiments and CD-MUSIC Modeling. *Chemosphere* **2011**, *82*, 1475−1481.

(15) Goldberg, S.; Glaubig, R. A. Boron Adsorption on Aluminum and Iron Oxide Minerals 1. *Soil Sci. Soc. Am. J.* **1985**, *49*, 1374−1379.

(16) Su, C.; Suarez, D. L. Coordination of Adsorbed Boron: A FTIR Spectroscopic Study. *Environ. Sci. Technol.* **1995**, *29*, 302−311.

(17) Peak, D.; Luther, G. W.; Sparks, D. L. ATR-FTIR Spectroscopic Studies of Boric Acid Adsorption on Hydrous Ferric Oxide. *Geochim. Cosmochim. Acta* **2003**, *67*, 2551−2560.

(18) Kurokawa, R.; Kamura, K. Adsorption of Boron by Volcanic Ash Soils Distributed in Japan. *Soil Sci. Soc. Am. J.* **2018**, *82*, 671−677.

(19) Jambor, J. L.; Dutrizac, J. E. Occurrence and Constitution of Natural and Synthetic Ferrihydrite, a Widespread Iron Oxyhydroxide. *Chem. Rev.* **1998**, *98*, 2549−2585.

(20) Groenenberg, J. E.; Lofts, S. The Use of Assemblage Models to Describe Trace Element Partitioning, Speciation, and Fate: A Review. *Environ. Toxicol. Chem.* **2014**, *33*, 2181−2196.

(21) Dzombak, D. A.; Morel, F. M. M. *Surface Complexation Modeling: Hydrous Ferric Oxide*; John Wiley & Sons, 1990.

(22) Goldberg, S. Reanalysis of Boron Adsorption on Soils and Soil Minerals Using the Constant Capacitance Model. *Soil Sci. Soc. Am. J.* **1999**, *63*, 823−829.

(23) Goldberg, S. Use of Surface Complexation Models in Soil Chemical Systems. *Adv. Agron.* **1992**, *47*, 233−329.

(24) Stern, O. Zur Theorie Der Elektrolytischen Doppelschicht. *Z. Elektrochem. Angew. Phys. Chem.* **1924**, *30*, 508−516.

(25) Hiemstra, T.; Van Riemsdijk, W. H. A Surface Structural Approach to Ion Adsorption: The Charge Distribution (CD) Model. *J. Colloid Interface Sci.* **1996**, *179*, 488−508.

(26) Hiemstra, T.; Zhao, W. Reactivity of Ferrihydrite and Ferritin in Relation to Surface Structure, Size, and Nanoparticle Formation Studied for Phosphate and Arsenate. *Environ. Sci. Nano* **2016**, *3*, 1265−1279.

(27) Mendez, J. C.; Hiemstra, T. Surface Area of Ferrihydrite Consistently Related to Primary Surface Charge, Ion Pair Formation, and Specific Ion Adsorption. *Chem. Geol.* **2020**, *532*, No. 119304.

(28) Michel, F. M.; Ehm, L.; Antao, S. M.; Lee, P. L.; Chupas, P. J.; Liu, G.; Strongin, D. R.; Schoonen, M. A. A.; Phillips, B. L.; Parise, J. B. The Structure of Ferrihydrite, a Nanocrystalline Material. *Science* **2007**, *316*, 1726−1729.

(29) Hiemstra, T. Surface and Mineral Structure of Ferrihydrite. *Geochim. Cosmochim. Acta* **2013**, *105*, 316−325.

(30) Hiemstra, T. Surface Structure Controlling Nanoparticle Behavior: Magnetism of Ferrihydrite, Magnetite, and Maghemite. *Environ. Sci. Nano* **2018**, *5*, 752−764.

(31) Bompoti, N.; Chrysochoou, M.; Machesky, M. Surface Structure of Ferrihydrite: Insights from Modeling Surface Charge. *Chem. Geol.* **2017**, *464*, 34−45.

(32) Hiemstra, T.; Mendez, J. C.; Li, J. Evolution of the Reactive Surface Area of Ferrihydrite: Time, PH, and Temperature Dependency of Growth by Ostwald Ripening. *Environ. Sci. Nano* **2019**, *6*, 820−833.

(33) Davis, J. A.; Leckie, J. O. Surface Ionization and Complexation at the Oxide/Water Interface II. Surface Properties of Amorphous Iron Oxyhydroxide and Adsorption of Metal Ions. *J. Colloid Interface Sci.* **1978**, *67*, 90−107.

(34) Weidler, P. G. BET Sample Pretreatment of Synthetic Ferrihydrite and Its Influence on the Determination of Surface Area and Porosity. *J. Porous Mater.* **1997**, *4*, 165−169.

(35) van der Giessen, A. A. The Structure of Iron (III) Oxide-Hydrate Gels. *J. Inorg. Nucl. Chem.* **1966**, *28*, 2155−2159.

(36) Brown, I. D.; Altermatt, D. Bond-valence Parameters Obtained from a Systematic Analysis of the Inorganic Crystal Structure Database. *Acta Crystallogr., Sect. B: Struct. Sci.* **1985**, *41*, 244−247.

(37) Brown, I. D. Recent Developments in the Methods and Applications of the Bond Valence Model. *Chem. Rev.* **2009**, *109*, 6858−6919.

(38) Mendez, J. C.; Hiemstra, T. Carbonate Adsorption to Ferrihydrite: Competitive Interaction with Phosphate for Use in Soil Systems. *ACS Earth Space Chem.* **2018**, *3*, 129−141.

(39) Hiemstra, T. Ferrihydrite Interaction with Silicate and Competing Oxyanions: Geometry and Hydrogen Bonding of Surface Species. *Geochim. Cosmochim. Acta* **2018**, *238*, 453−476.
(40) Mendez, J. C.; Hiemstra, T. High and Low Affinity Sites of Ferrihydrite for Metal Ion Adsorption: Data and Modeling of the Alkaline-Earth Ions Be, Mg, Ca, Sr, Ba, and Ra. *Geochim. Cosmochim. Acta*, 2020.
(41) Mendez, J. C.; Hiemstra, T. Ternary Complex Formation of Phosphate with Ca and Mg Ions Binding to Ferrihydrite: Experiments and Mechanisms. *ACS Earth Space Chem.* **2020**, *4*, 545−557.
(42) Lemarchand, E.; Schott, J.; Gaillardet, J. How Surface Complexes Impact Boron Isotope Fractionation: Evidence from Fe and Mn Oxides Sorption Experiments. *Earth Planet. Sci. Lett.* **2007**, *260*, 277−296.
(43) Kim, Y.; Kirkpatrick, R. J. 11B NMR Investigation of Boron Interaction with Mineral Surfaces: Results for Boehmite, Silica Gel and Illite. *Geochim. Cosmochim. Acta* **2006**, *70*, 3231−3238.
(44) Goli, E.; Hiemstra, T.; Rahnemaie, R. Interaction of Boron with Humic Acid and Natural Organic Matter: Experiments and Modeling. *Chem. Geol.* **2019**, *515*, 1−8.
(45) Tiberg, C.; Sjöstedt, C.; Persson, I.; Gustafsson, J. P. Phosphate Effects on Copper(II) and Lead(II) Sorption to Ferrihydrite. *Geochim. Cosmochim. Acta* **2013**, *120*, 140−157.
(46) Hiemstra, T.; Van Riemsdijk, W. H. On the Relationship between Charge Distribution, Surface Hydration, and the Structure of the Interface of Metal Hydroxides. *J. Colloid Interface Sci.* **2006**, *301*, 1−18.
(47) Hiemstra, T.; Van Riemsdijk, W. H. A Surface Structural Model for Ferrihydrite I: Sites Related to Primary Charge, Molar Mass, and Mass Density. *Geochim. Cosmochim. Acta* **2009**, *73*, 4423−4436.
(48) Keizer, M. G.; Van Riemsdijk, W. H. *ECOSAT, a Computer Program for the Calculation of Chemical Speciation and Transport in Soil−Water Systems*; Wageningen Agricultural University: Wageningen, The Netherlands, 1995.
(49) Kinniburgh, D. G. *FIT User Guide*, Technical Report WD/93/23; British Geological Survey: Keyworth, 1993.
(50) Hiemstra, T.; Antelo, J.; Rahnemaie, R.; van Riemsdijk, W. H. Nanoparticles in Natural Systems I: The Effective Reactive Surface Area of the Natural Oxide Fraction in Field Samples. *Geochim. Cosmochim. Acta* **2010**, *74*, 41−58.
(51) Dijkstra, J. J.; Meeussen, J. C. L.; Comans, R. N. J. Evaluation of a Generic Multisurface Sorption Model for Inorganic Soil Contaminants. *Environ. Sci. Technol.* **2009**, *43*, 6196−6201.
(52) Groenenberg, J. E.; Römkens, P. F. A. M.; Van Zomeren, A.; Rodrigues, S. M.; Comans, R. N. J. Evaluation of the Single Dilute (0.43 M) Nitric Acid Extraction to Determine Geochemically Reactive Elements in Soil. *Environ. Sci. Technol.* **2017**, *51*, 2246−2253.
(53) Weng, L.; Temminghoff, E. J. M.; Van Riemsdijk, W. H. Contribution of Individual Sorbents to the Control of Heavy Metal Activity in Sandy Soil. *Environ. Sci. Technol.* **2001**, *35*, 4436−4443.
(54) Duffner, A.; Weng, L.; Hoffland, E.; van der Zee, S. E. A. T. M. Multi-Surface Modeling to Predict Free Zinc Ion Concentrations in Low-Zinc Soils. *Environ. Sci. Technol.* **2014**, *48*, 5700−5708.
(55) Degryse, F.; Broos, K.; Smolders, E.; Merckx, R. Soil Solution Concentration of Cd and Zn Canbe Predicted with a CaCl 2 Soil Extract. *Eur. J. Soil Sci.* **2003**, *54*, 149−158.
(56) Novozamsky, I.; Barrera, L. L.; Houba, V. J. G.; van der Lee, J. J.; van Eck, R. Comparison of a Hot Water and Cold 0.01 M $CaCl_2$ Extraction Procedures for the Determination of Boron in Soil. *Commun. Soil Sci. Plant Anal.* **1990**, *21*, 2189−2195.
(57) Milne, C. J.; Kinniburgh, D. G.; van Riemsdijk, W. H.; Tipping, E. Generic NICA−Donnan Model Parameters for Metal-Ion Binding by Humic Substances. *Environ. Sci. Technol.* **2003**, *37*, 958−971.
(58) Tiberg, C.; Sjöstedt, C.; Gustafsson, J. P. Metal Sorption to Spodosol Bs Horizons: Organic Matter Complexes Predominate. *Chemosphere* **2018**, *196*, 556−565.
(59) Rietra, R. P. J. J. J.; Hiemstra, T.; van Riemsdijk, W. H. The Relationship between Molecular Structure and Ion Adsorption on Variable Charge Minerals. *Geochim. Cosmochim. Acta* **1999**, *63*, 3009−3015.
(60) Perona, M.; Leckie, J. Proton Stoichiometry for the Adsorption of Cations on Oxide Surfaces. *J. Colloid Interface Sci.* **1985**, *106*, 64−69.
(61) Xu, D.; Peak, D. Adsorption of Boric Acid on Pure and Humic Acid Coated Am-Al(OH)3: A Boron K-Edge XANES Study. *Environ. Sci. Technol.* **2007**, *41*, 903−908.
(62) Hiemstra, T.; Van Riemsdijk, W. H.; Rossberg, A.; Ulrich, K.-U. A Surface Structural Model for Ferrihydrite II: Adsorption of Uranyl and Carbonate. *Geochim. Cosmochim. Acta* **2009**, *73*, 4437−4451.
(63) Brown, I. D.; Altermatt, D. Bond-Valence Parameters Obtained from a Systematic Analysis of the Inorganic Crystal Structure Database. *Acta Crystallogr., Sect. B: Struct. Sci.* **1985**, *41*, 244−247.
(64) Benjamin, M. M.; Leckie, J. O. Multiple-Site Adsorption of Cd, Cu, Zn, and Pb on Amorphous Iron Oxyhydroxide. *J. Colloid Interface Sci.* **1981**, *79*, 209−221.
(65) Swedlund, P.; Webster, J. Cu and Zn Ternary Surface Complex Formation with SO4 on Ferrihydrite and Schwertmannite. *Appl. Geochem.* **2001**, *16*, 503−511.
(66) Tiberg, C.; Gustafsson, J. P. Phosphate Effects on Cadmium(II) Sorption to Ferrihydrite. *J. Colloid Interface Sci.* **2016**, *471*, 103−111.
(67) Gu, B.; Lowe, L. E. Studies on te Ad Sorption of Boron on Humic Acids. *Can. J. Soil Sci* **1990**, *70*, 305−311.
(68) Majidi, A.; Rahnemaie, R.; Hassani, A.; Malakouti, M. J. Adsorption and Desorption Processes of Boron in Calcareous Soils. *Chemosphere* **2010**, *80*, 733−739.

https://dx.doi.org/10.1021/acsearthspacechem.0c00078
ACS Earth Space Chem. 2020, 4, 1269−1280